Journal Pre-proof

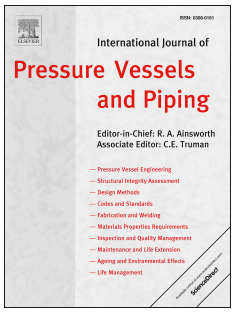

Assessment of corroded API 5L X52 pipe elbow using a modified failure assessment diagram

Bassam Gamal Nasser Muthanna, Omar Bouledroua, Madjid Meriem-Benziane, Mahdi Razavi Setvati, Milos B. Djukic

PII: S0308-0161(20)30266-0

DOI: https://doi.org/10.1016/j.ijpvp.2020.104291

Reference: IPVP 104291

To appear in: *International Journal of Pressure Vessels and Piping*

Received Date: 1 October 2020

Revised Date: 19 December 2020

Accepted Date: 22 December 2020

Please cite this article as: Nasser Muthanna BG, Bouledroua O, Meriem-Benziane M, Setvati MR, Djukic MB, Assessment of corroded API 5L X52 pipe elbow using a modified failure assessment diagram, *International Journal of Pressure Vessels and Piping* (2021), doi: https://doi.org/10.1016/j.ijpvp.2020.104291.

Author Statement

Corresponding author: Bassam Gamal Nasser Muthanna

As corresponding author, I am responsible for ensuring that the descriptions are accurate and agreed by all authors. I inform you that all authors have contributed in this project.

Title of Paper

Assessment of corroded API 5L X52 pipe elbow using a modified failure assessment diagram

Authors name:

Bassam Gamal Nasser Muthanna,

Omar Bouledroua,

Madjid Meriem-Benziane,

Mahdi Razavi Setvati,

Milos B. Djukic

Assessment of corroded API 5L X52 pipe elbow using a modified failure assessment diagram

Bassam Gamal Nasser Muthanna[1*], Omar Bouledroua[2], Madjid Meriem-Benziane[1], Mahdi Razavi Setvati[3], Milos B. Djukic[4]

[1] *LRM, Faculty of Technology, Hassiba Benbouali University of Chlef, Esalem City, 02000, Chlef, Algeria.*
[2] *LPTPM, Hassiba BenBouali University of Chlef, P.O.Box. 151 Hay Salem, 02000 Chlef, Algeria.*
[3] *Faculty of Technology, Design and Environment, Oxford Brookes University, Oxford, United Kingdom.*
[4] *University of Belgrade, Faculty of Mechanical Engineering, Kraljice Marije 16, Belgrade 11120, Serbia.*

***E-mail*:** b.muthanna@univ-chlef.dz; bassam.gamal36@gmail.com

Abstract:

Pipe elbows (bends) are considered critical pressurized components in the piping systems and pipelines due to their stress intensification and the effect of bend curvature. They are prone and hence more exposed to different corrosion failure modes than straight pipes. Late detection of such elbow damages can lead to different dangerous and emergency situations which cause environmental disasters, pollution, substantial consumer losses and a serious threat to human life. A comprehensive safety and reliability assessment of pipe elbows, including usage of prediction models, can provide significant increases in the service life of pipelines. It is well known that the limit pressure is an important parameter to assess the piping integrity. In this paper, the integrity assessment of damaged pipeline elbows made of API 5L X52 steel was done within the framework of numerical modeling using the finite element method (FEM) and finite element analysis (FEA). The evaluation of numerically FEM modeled limit pressure in the corroded elbow containing a rectangular parallelepiped-shaped corrosion defect with rounded corners at the intrados section was done and compared to different codes for calculating limit pressure. Moreover, the area with the corrosion defects with different relative defect depth to wall thickness ratios was FEM modeled at the intrados section of the pipe elbow where the highest hoop stress exists. The results showed that the codes for straight pipes could not be applied for the pipe elbows due to the significantly higher error in the obtained limit pressure value compared with numerically FEM obtained results. However, the results for modified codes, adapted for the pipe elbow case using the Goodall formula for calculation of the hoop stress in pipe elbows with defects are pretty consistent with the numerical FEA results. The notch failure assessment diagram (NFAD) was also used for the straight pipe and pipe bends with different corrosion defect depth ratios, while the obtained critical defect depth ratios further highlighted the criticality of pipe elbows as an essential pipeline component.

Keywords: Pipe elbow, Corrosion, Limit pressure, Codes, FEA.

1. Introduction

In the hydrocarbons processing industry, pipelines are essential components to transport energy in the safest way in large volumes over large distances. Consequently, the structural integrity, high reliability, and effective maintenance of pipelines take the highest importance due to the critical role of pipelines in global economic and environmental safety. In recent decades, the use of crude oil and natural gas has increased faster which leads to the need for modifications, implementation of improved maintenance strategies, and extension of existing pipeline systems. This complicated network of pipelines includes the necessity for usage of numerous and various pipe elbows (bends) and junctions for distribution, transportation, and change of the fluid direction. The pipe elbows are prone to the various damage mechanisms on both internal and external surfaces due to the exposure to fluids and external environments such as corrosion, erosion, erosion-corrosion fatigue, and different other combined damages [1-14]. Frequently this leads to the burst in critical parts of piping systems, forced outages, and long term interruptions in operation. The corrosion of pipe elbows in natural gas pipelines and various other industrial systems such as hydrocarbons industries and desalination plants [15-19] was extensively examined and reported.

Extensive studies have been conducted related to the reliability and structural integrity prediction, prevention of corrosion damages, and repair of corroded steel pipelines and pipe elbows [20-37]. Different experimental approaches and tests, numerical analyses, and analytical methods were used. Knowledge of limit pressure (P_L) is an important issue in the field of pipeline design, integrity assessment, and maintenance management to achieve prolonged and reliable operation of pipelines [38,39]. Generally, failure pressure appears when the internal pipeline pressure exceeds the limit pressure value [40,41]. NG-18 equation was the first original formula and the semi-empirical failure criteria developed by Maxey et al. [42] to calculate the residual strength of corroded straight pipes with cracks and defects. However, there are various models, standards, codes, and plastic collapse failure criteria based on NG-18 equations [42] such as ASME B31G [43], modified ASME B31G [44], DNV-RP-F101 [45], Shell-92 [46], RSTRENG [47], and PCORRC [48] which were developed to calculate the limit pressure according to the flow stress in the straight pipe. However, these standards and codes for the fitness-for-purpose assessment of corroded pipelines could not be applied to pipe elbows due to the effect of the elbow curvature that leads to the increase of hoop stress [49].

Some researchers [23,32,33,50] have proposed new formulas to calculate the limit pressure for a pipe elbow with the defects. Goodall [51] has proposed the first formula to calculate the circumferential stress in pipe elbows with defects. This formula is presented later in section 2. Various authors have performed their analysis on the plastic limit pressure of elbows and proposed different models based on the Goodall formula [32,49]. Duan and Shen [32] have proposed an empirical model for the calculation of the limit load in pipe elbows at the extrados location and also validated by experiments. Yahiaoui et al. [50] have studied the elbows with a short radius and cracks by using FEM. Kim et al. [52] have examined the integrity of a pipe elbow in the presence of defects at the intrados and extrados sections under internal pressure and plane-bending load. They have concluded that the intrados section is more endangered and vulnerable than the extrados section according to their experiments and obtained results. Lee et al. [33] have studied erosion-corrosion provoked defects in different positions of the pipe elbow using mathematical formulas and numerical analysis. They proposed a new method to calculate burst pressure using industrial codes and the Lorenz factor [33]. Xie et al. [23] have proposed a new formula by introducing curvature and wall thickness factors to calculate hoop stress in the thick-walled elbow, which was additionally verified and supported using the FEM. Tee and Wordu [53] have found that the geometrical parameters of the corrosion defect (length and depth) have a significant influence on the failure pressure. Besides, the shape of the gouge has more impact than the shape of a corrosion pit.

The fracture mechanics is considered as important during the evaluation of the structural integrity of piping systems. Based on the theory of linear elastic fracture mechanics (LEFM), failure occurs when the value of the stress intensity factor (K_I) is higher than the critical value of plane strain fracture toughness for mode I crack displacement (K_{IC}), i.e., ($K_I \geq K_{IC}$) [54].

The localized (pitting) corrosion generally considered as a notch in the piping system. The notch has a strong influence on the failure or burst and the Notch Stress Intensity Factor (NSIF) is used as a prediction for the fracture concept [55-57]. Depending on the notch term, the failure occurs when the stress distribution exceeds the critical value at the notch tip ($K_{\bullet} \geq K_{\bullet C}$). The critical NSIF could be called fracture toughness ($K_{\bullet C}$) in notch tips. Furthermore, the constraint has a significant effect on the fracture toughness value [58,59]. The volumetric method is used in order to calculate NSIF. It is considered a semi-local method for numerical analysis [60-62].

The Notch Failure Assessment Diagram (NFAD) is frequently used to study the safety and for the fracture assessment of pipelines or elbows with different types of defects [39,41,63-76]. It depends on the fracture toughness (K_{mat}), defect size, i.e., defect depth ratio *(d/t)*, and the internal loading - pressure *(P)* [69]. The NFAD methodology substituted these three parameters with only two non-dimensional parameters K_r and L_r, which present the applied stress and the crack driving force, respectively, and by introducing the corresponding assessment point coordinates (L_r, K_r) on the FAD and NFAD [69]. Numerous previous studies have shown that elbows are more vulnerable than straight pipes due to the more severe stress conditions of elbows with a defect, while assessment points for elbows are typically shifted in comparison with straight pipes and located in the brittle fracture domain of the FAD or NFAD (see subsection 3.3.) [17,52,63-65].

In our previous study [12], the critical position along a pipe elbow made of API 5L X52 steel, according to the effects of the critical stress location, critical crack orientation angle, and critical elbow angle on SIF, was investigated with the aid of a modified FAD [12]. The critical position along the elbow with the maximum stress was located at a curvature angle α= 72°. Also, a semi-elliptical crack was created at this location, at the critical intrados section of pipe elbow [52], taken into account the importance of equivalent stress intensity factor (K_{eq}) as a failure criterion to determine the critical semi-elliptical crack angle orientation. The crack orientation angle of 90° was found to be critical for a pipe elbow [12]. It was also observed that due to stress intensification and higher constraint in pipe elbows, the corresponding assessment point for the same relative defect size located at the intrados section of pipe elbow has a higher value of both coordinates (L_r, K_r) then for the straight pipe.

In this work, the rectangular parallelepiped-shaped corrosion defects with rounded corners without crack and with different relative defect depth to wall thickness ratios (d/t= 0.1 - 0.8, see Fig. 1c) at the middle of the critical [52] intrados section of a pipe elbow (API 5L X52 steel) were created to examine the effects of corrosion defects on the integrity assessment of pipe elbows. The limit pressure prediction for a pipe elbow containing corrosion defects at the intrados section is investigated using FEA. For limit pressure calculation in the pipe elbow with different defect depth ratios and to check the applicability of modified codes, the Goodall formula [52] for calculation of the hoop stress (σ_h) in pipe elbow was used in various codes. The obtained results were further compared with the numerical FEA results, and consequently, the applicability of different modified codes (adapted for the pipe elbow case) for the calculation of the limit pressure in the pipe elbow was also checked. The notch failure

assessment diagram (NFAD) is used for the straight pipe and pipe bends for the safety factor calculation and to evaluate the critical detect depth ratios. Finally, the obtained results of the structural integrity assessment for pipe elbows with different relative corrosion defect depth ratios presented in this study are compared with our previously published results [12] for a pipe elbow with different semi-elliptical relative crack depth ratios.

2. Limit pressure standards and pipe elbow hoop stress

In the literature, several codes have been successfully used as failure criteria for the reliability assessment of corroded pipelines [43-48,75]. Cosham et al. [75] have pointed out that the applicability of a particular code strongly depends on the toughness value of different pipeline steels. The older models, like ASME B31G [43], modified ASME B31G [44], and the remaining strength formula - RSTRENG [47], were developed and validated through tests on older pipeline steels with relatively lower toughness. On the other hand, the new models, like DNV-RP-F101 [45], and PCORRC [48], are mostly based on equations following both numerical - finite element analyses (FEA) and experimental data. These "new" models were developed and validated for high toughness pipeline steels, and hence suitable and applicable mostly for these modern steels [75]. Also, Cosham et al. [75] emphasized that some of the methods for assessing corrosion based on the NG-18 equations [42], particularly older ASME B31G [43] and modified B31G [44], are rather conservative in the case of blunt, part-wall defects.

Various codes and standards for the straight pipe have a detailed form and style for their formulas and applied deterministic approaches, Table 1. The main stresses (stress components) for the straight pipe subjected to internal pressure are expressed by the following equations [77]:

$$\bullet_{\cdot} = \frac{Pr}{t} \quad , \quad \bullet_{l} = \frac{Pr}{2t} = 0.5 \bullet_{\cdot} \quad , \quad \bullet_{r} \bullet 0 \tag{1}$$

where, $\bullet_{\cdot}$, $\bullet_{l}$, $\bullet_{r}$, P, r, and t are hoop stress, longitudinal stress, radial stress, internal pressure, average radius and wall thickness of pipeline, respectively. According to the deterministic assessment models, both older and contemporary models mentioned above, the internal pressure (P) must be less than the limit pressure (P_L): ($P < P_L$) to prevent the pipe burst, Table 1. For corroded pipes made of old steels with lower toughness, limit pressure can be calculated using one of the standard but older models (ASME B31G, Modified ASME

B31G, and RSTRENG). For the modern steels with higher toughness, limit pressure can be calculated using one of the contemporary models (DNV RP-F101 and PCORRC) [78,79].

Table 1 Codes for calculating limit pressure P_L of the straight pipe.

The parameters presented in Table 1: P_L, D, d, t, M, σ_y, σ_{ult}, and L are the limit pressure, pipe outer diameter, crack depth, wall thickness, Folias factor, yield strength, ultimate tensile strength, and longitudinal corrosion defect length, respectively. Hoop stress is the dominant stress for pipelines subjected to internal pressure, and the parameters d and L are important input parameters for the limit pressure - P_L based models. The main difference between codes presented in Table 1 is the definition of the flow stress σ_0 (based on σ_y or σ_{ult}) and the defect shape [75]. ASME B31G [43] code is used for the parabolic shape corrosion defects, while the maximum hoop stress cannot exceed the yield strength of the material $\sigma_h \leq \sigma_y$. The modified ASME B31G [44] model is used for the idealized, rectangular in shape corrosion defects while the total defect depth should not exceed 80 % of the wall thickness [33]. Shell-92 [46], PCORRC [47], and DNV RP-F101 [45] models are also used for the rectangular shape defects and they are applicable in the case of blunt defects in tough materials [78,79].

The hoop stress in the pipelines subjected to internal pressure is different from that of the pipe elbow. It occurs in a circumferential direction. On the contrary, the longitudinal stress is the same for both straight pipe and pipe elbow, hence the presence of curvature of the elbow does not influence the longitudinal stress [80]. The hoop stress at the extrados section of the pipe elbow is the lowest, while the intrados section is the zone of the highest hoop stress [80]. The increase of bend radius causes an increase in the hoop stress at the extrados section, while at the intrados section the hoop stress is diminishing [25]. The different hoop stress equations were proposed in the literature for a pressurized pipe elbow and presented by Goodall [51] - Eq. (2), Li et al. [25] - Eq. (3), and Xie et al. [23] - Eq. (4), respectively:

$$\sigma_h = \frac{Pr}{t} \cdot \frac{1 \cdot r/2R}{1 \cdot r/R} \tag{2}$$

$$\sigma_h = \frac{Pr}{2t} \cdot \frac{2R + r\sin\theta}{R + r\sin\theta} \tag{3}$$

$$\sigma_h = \frac{Pr}{t} \cdot C_t \cdot C_R = \frac{Pr}{t} \cdot 0.5 \cdot \left[1 + \left(\frac{D}{2r}\right)^2\right] \cdot \left[\left(1 \cdot \frac{t}{D}\right)^2\right] \cdot \left[1 \cdot \frac{1}{2\left(1 + \frac{2R}{D\sin\theta}\right)}\right] \tag{4}$$

where, P, r, t, R, D, C_t, C_R, *and* (r, •) are the internal pressure, mean radius, wall thickness, bend radius, outer diameter, wall thickness factor, curvature factor of pipe elbow, and coordinates of calculated points, respectively. Equation (4), proposed by Xie et al. [23] also included two additional correction factors, i.e., the wall thickness factor C_t and curvature factor C_R. Miller [81] pointed out the conservatism related to the Goodall formula (Eq. (2)), predominantly due to the absence of experimental validation.

3. Results and discussions

This research represents a continuation and further advancement regarding our previous studies and conclusions about the integrity assessment of damaged pipeline elbows. In our previous research [16], the comprehensive case study of corroded pipe elbows due to the fluid-solid interaction under the complex operating conditions and the presence of silicone particles was done. In recent work, the numerical FEA study of semi-elliptical cracks in the critical position at the intrados section of the pipe elbow was conducted [12]. The applicability of different codes for calculations of the limit pressure in the corroded straight pipes in the presence of various fluid flow conditions (pure natural gas and natural gas-hydrogen mix transport) were also examined and compared with the FEA results [41,66,67,70,76].

This study is carried out by using a finite element analysis (FEA) to simulate a pipe elbow with the rectangular parallelepiped-shaped corrosion defects with rounded corners and with different relative defect depth to wall thickness ratios (d/t= 0.1 - 0.8, see Fig. 1c) at the critical intrados section of the pipe elbow. The numerical FEA results were also compared with results obtained by codes to modify the limit pressure equations of codes (ASME B31G, modified ASME B31G, and DNV RP-F101), presented in Table 1. The modification includes the implementation of the Goodall formula (Eq. (2)) for the hoop stress •. in the pipe elbow during the calculation of the limit pressure P_L according to three codes originally developed for the straight pipe.

For this reason, all results and discussions are presented in three subsections. First, in subsection 3.1, the hoop stress at the intrados location of the pipe elbow without defect was examined and calculated using the equations suggested in the literature for the straight pipe (Eq. (1)) and Goodall formula for the pipe elbow (Eq. (2)). Also, these results are compared with the results for the distribution of hoop stress on the intrados (• = 0°) sections of the pipe elbow obtained by numerical FEA. In the next subsection 3.2, the results of the limit pressure

calculation for different corrosion defect depth ratios using three modified codes (ASME B31G, modified ASME B31G, and DNV RP-F101), and the Goodall formula [51] for calculation of the hoop stress ($\bullet$.) in the pipe elbow, is presented and compared with numerical FEA results. Also, the NFAD for the straight pipe and pipe bends with corrosion defects for the safety factor calculation is presented and further analyzed in the final subsection 3.3.

3.1. Hoop stress at intrados section of the pipe elbow without defect, models and FEA results

The numerical study was conducted using the FEA software ANSYS [82]. A pipe elbow made of API X52 pipeline steel was used in this work and its dimensions are shown in Fig. 1. Table 2 presents the mechanical properties of the pipe elbow made of API 5L X52 steel.

Fig. 1. API X52 pipeline elbow: (a) manifold separation system; (b) corroded pipe elbow; (c) pipe elbow dimensions.

Figs. 1a and 1b show the intake manifold elbows connected with the horizontal three-phase separators. The geometrical characteristics of the pipe elbow are the internal radius r= 285.75 mm, wall thickness t= 12.7 mm, the length L= 1000 mm, and the bending radius R= 798.45 mm, Figs. 1b and 1c.

Table 2 Mechanical properties of API 5L X52 pipeline steel.

A pipe elbow is subjected to the internal - service pressure P_s= 7 MPa. The FEM results are shown in Fig. 2. Fig. 2a shows the 90° pipe elbow geometry. Fig. 2b shows the mesh constructed with a 16-node quadrilateral element available in ANSYS software. Fig. 2c illustrates the hoop stress distribution along the pipe elbow. Fig. 3a presents the distribution of hoop stresses at different angles along the pipe elbow, as illustrated in Fig. 3b.

Fig. 2. Pipe elbow without corrosion defects subjected to the internal - service pressure P_s= 7 MPa, geometry, meshing, and hoop stress distribution.

Fig. 3. Pipe elbow without corrosion defects: (a) distribution of the hoop stress; (b) different paths angles along the pipe elbow.

It is clear that the maximal value of hoop stress is located at the intrados section of the pipe elbow, as shown in Figs. 2 and 3. Figs. 3a and 3b present the distribution of hoop stress at the intrados ($\bullet$ = 0°), extrados ($\bullet$ = 180°) and crown ($\bullet$ = 90°) sections of the pipe elbow.

Moreover, results confirm the critical influence of the intrados section of the pipe elbow based on the obtained high hoop stress value that equals σ_h = 212.4 MPa. The value of hoop stress decreases at the crown section of the pipe elbow, and it is close to the value for the straight pipe (σ_h = 164.5 MPa).

Table 3 Hoop stress σ_h at the intrados section of the pipe elbow without corrosion defects.

Table 3 shows the maximal hoop stress values obtained by the numerical FEA model together with values obtained using the Goodall formula (Eq. (2)), and the formula for the straight pipe (Eq. (1)). It is clear that the hoop stress value obtained using the Goodall formula - Eq. (2) (σ_h=201.39 MPa) is close to the value obtained by the numerical FEA model, Fig. 3 (σ_h=212.69 MPa), with the small error of 5.32 %, Table 3. The error is calculated using the following formula: error (%) = ($\sigma_{h\,(FEA)}$ - $\sigma_{h\,(Eq.1,\,2)}$) / $\sigma_{h\,(FEA)}$ x 100 %, where $\sigma_{h\,(FEA)}$, and $\sigma_{h\,(Eq.1,\,2)}$ are the hoop stress values obtained by FEM model, equation (1), and Eq. (2), respectively. On the other hand, a much higher error (25.94 %) is obtained using the straight pipe formula (Eq. (1)) for calculation of the hoop stress (σ_h=157.50 MPa), Table 3. Such a large discrepancy between hoop stress values at the intrados section of the pipe elbow, obtained by both FEA and the Goodall formula, and the value obtained using the formula for the straight pipes indicate the high criticality of this section of pipe elbows. A good agreement between the hoop stress value obtained using the Goodall formula [51] for calculation of the hoop stress (σ_h) in a pipe elbow, and the value obtained by numerical FEA model (see Table 3, error = 5.32 %), provides a solid background for checking the limit pressure calculations results using three modified codes. Also, the obtained numerical FEA value for the hoop stress ($\sigma_{h\,(FEA)}$= 212.69 MPa) as well as the error in comparison with the Goodall formula [51] results (5.32 %) are in close agreement with the maximum error of 6.58 % reported by Duan and Shen [32]. Once again, the hoop stress value obtained by the Goodall formula is somewhat higher than that obtained by the numerical FEA. The comparison of results obtained using modified codes and the FEA results is the topic of the next subsection 3.2.

3.2. The limit pressure calculation using modified codes and FEA results

In this subsection, the corroded pipe elbow assessment is studied to prevent their burst and the results of the limit pressure calculation using modified codes are compared with the FEA results. Previous research indicates that there is a serious need to determine a perfect formula

to calculate a limit pressure at the intrados section of the pipe elbow [23,25,32,33,50-52]. Therefore, the limit pressure of the corroded pipe elbow is analyzed using FEA and ANSYS software, as shown in Figs. 4 and 5. The rectangular parallelepiped-shaped corrosion defect with rounded corners is simulated at the intrados section of the pipe elbow. The pipe elbow with a length (L= 174 mm), width (W= 208 mm), and with different geometrical relative corrosion defect depth to wall thickness ratios (d/t= 0.1 - 0.8, see Fig. 1c) is investigated, Fig.4. The corrosion defects with different d/t depth ratios were modeled at the intrados section of the 90° pipe elbow, Figs. 4a and 4b. The hoop stress distribution for d/t= 0.5 is shown in Fig. 4c.

Fig. 4. Pipe elbow with the rectangular parallelepiped-shaped corrosion defect with rounded corners at the intrados section subjected to the internal - service pressure P_s= 7 MPa: pipe elbow and the geometry of rectangular parallelepiped-shaped corrosion defect with rounded corners, meshing, and hoop stress distribution (d/t= 0.5).

In conducted FEA, for each defect depth (d/t= 0.1 - 0.8, see Fig. 1c), the applied pressure is increased with an increment of 1 MPa, from 1 MPa to the maximal 16 MPa. The hoop stress that is equal to the yield or ultimate strength can be considered as a limit pressure, as indicated in Fig. 5a. The effects of defect depth ratios (d/t= 0.1 - 0.8) on the hoop stress were analyzed at different internal pressures. Below the yield strength value (σ_y= 410 MPa), a typical linear increase of the hoop stress can be observed, Fig 5a [76]. Due to the entering into the plastic regime, above σ_y while approaching the ultimate strength value ($\bullet_{ult}$= 520 MPa), nonlinearity in the hoop stress increase was observed, Fig 5a. Fig. 5b illustrates the numerical FEA obtained limit pressures based on the yield σ_y and ultimate strength $\bullet_{ult}$ values for API 5L X52 steel with different defect depth ratios (d/t= 0.1 - 0.8, see Fig. 1c) at the intrados section of the pipe elbow.

Fig. 5. Numerical analysis of elbow defects with different depth ratios d/t at the intrados section: (a) hoop stress versus internal pressure; (b) limit pressure P_L according to the yield and ultimate strength.

As previously discussed, the limit pressure determines the pipe burst. It depends on two main mechanical properties (i) yield strength σ_y and (ii) ultimate strength $\bullet_{ult}$. As indicated in Figs. 5a and 5b, the limit pressure for the pipe elbow made of API 5L X52 steel with defect depth ratio d/t= 0.1 is almost 16 MPa based on the ultimate strength and 12 MPa based on the

yield strength. While the limit pressure for defected pipe elbow with defect depth ratio d/t= 0.8 is much lower, approximately 8 MPa based on the ultimate strength and only 4.5 MPa based on the yield strength. The reduction of the internal - service pressure P_s= 7 MPa (Fig. 5b) in the pipe elbow is necessary when a critical defect depth reaches d/t= 0.65, based on the yield strength σ_y= 410 MPa for API 5L X52 steel. In this study of pipe elbows, the presented numerical FEA results (Figs. 5b and 6) indicate that the use of yield strength as a limit value for the limit pressure determination does not represent a conservative solution as it was in the case of straight pipe made of the same steel [76]. It is also important to note that in our previous study [66,76] the oval-shaped corrosion defects were introduced with the same defect depth ratios range (d/t= 0.1 - 0.8), while in this study more stress intensive rectangular parallelepiped-shaped corrosion defects with rounded corners are investigated. Nevertheless, during comparison of the suitability for application of the ultimate strength or yield strength as a limit value for the limit pressure determination and the conservatism estimation, it is necessary to take into account other important factors. These factors are (i) the pipeline component: straight pipe or a pipe elbow, (ii) the type of the defect: cracks (the stress intensity factor - SIF) or corrosion defects without the crack, (iii) geometrical characteristics of the corrosion defect (the degree of stress intensification), and (iv) the relative defect depth to wall thickness ratio d/t [12,16,38,39,41,66,69,72,76].

Finally, it is important to reduce the internal pressure when the defect size is increasing to maintain the reliable operation of pipelines. It is always advisable to make a comparison between the deterministic and probabilistic approaches because of the confirmed trend of a decrease in the reliability index with an increase of the defect depth to wall thickness ratio [76]. It is clear based on the presented results that pipe elbows represent critical components and hence endangered mostly the reliability of pipelines.

The comparison between the numerical FEA results for the limit pressure, and results obtained using three modified codes (ASME B31G, modified ASME B31G, and DNV RP-F101) for different corrosion defect depth ratios are presented in Fig. 6. The decrease of the limit pressure in API 5L X52 made steel pipeline is compared for the straight pipe case, using three standard codes, and for the pipe elbow case, using both modified codes together with the Goodall formula for calculation of the hoop stress in the pipe elbow and FEA results. The numerical FEA results for the limit pressure based on both yield strength and ultimate strength are presented in Fig. 6. The rectangular parallelepiped-shaped corrosion defects with rounded corners and with different corrosion defect depth ratios (d/t= 0.1 - 0.8) are located at

the straight pipe, and at the intrados section of the pipe elbow (Fig. 4), respectively. As expected, the limit pressure values in the straight pipe, obtained using all three codes, are significantly higher than for the pipe elbow. This indicates that the application of unmodified - original codes developed for the straight pipe in the case of the pipe elbow is not advisable and justified because of the significant overestimation of the allowable limit pressure.

Contrary, the results for the modified codes that take into account the pipe elbow geometry by using the Goodall formula for calculation of the hoop stress in the pipe elbow are found to be in close agreement with the numerical FEA results. When the ultimate strength is used to determine the limit pressure in the numerical FEA ($P_{L\,\bullet ult(FEA)}$), a much better agreement with results for all three modified standards are confirmed, Table 4. The maximal error within the range 10.56 % (d/t= 0.1) - 17.93 % (d/t= 0.8), (error (%)= ($P_{L\,(B31G)}$ - $P_{L\,\bullet ult(FEA)}$) / $P_{L\,\bullet ult(FEA)}$ x 100 %) is obtained using ASME B31G code for all defect depth ratios, Table 4. For defect depth ratios d/t below 0.5 ($d/t \leq 0.5$), the ASME B31G code calculation results are conservative (error: 1.40 % (d/t= 0.5) up to 10.56 % (d/t= 0.1)), and the gap between the FEA and ASME B31G results is diminishing while approaching the defect depth ratio of 0.5. At defect depth ratios higher than 0.5 ($d/t > 0.5$), the ASME B31G results for the limit pressure are higher than those obtained by the FEA (error: 4.39 % (d/t= 0.6) - 17.93 % (d/t= 0.8)), and the gap (error) becomes higher with further defect depth ratio increase up to d/t= 0.8, Table 4. A similar conservative trend when using the ASME B31G code was also observed by Lee et al. [33] and Amandi et al. [83]. The results for the limit pressure ($P_{L\,(Mod.\ B31G)}$ and $P_{L\,(DNV)}$) obtained using other two modified standards (modified ASME B31G, and DNV RP-F101) are less conservative, higher than those obtained by the FEA, and in better agreements with the numerical FEA results based on the ultimate strength ($P_{L\,\bullet ult(FEA)}$), see Fig. 6 and Table 4. The curvature of the FEA results and for both ASME B31G and DNV RP-F101 codes follow a similar trend. The results for both modified standards are slightly less conservative than FEA results and similarly for all defect depth ratios. A similar trend of the burst pressures values of the damaged pipe elbows obtained using ASME B31G and DNV RP-F101 codes was also observed by Lee et al. [33], albeit their study indicates that both models have shown more conservatism than the FEA.

The results obtained in this study using the modified ASME B31G standard ($P_{L\,(Mod.\ B31G)}$) are closest to the numerical FEA results ($P_{L\,\bullet ult(FEA)}$) for all defect depth ratios, Fig. 6. The error is relatively small for all depth ratios and within the range 2.49 - 10.27 %, Table 4. On the other hand, the numerical FEA results for the limit pressure in the pipe elbow using the

yield strength (P_L •$_{y(FEA)}$) for different defect depth ratios are consistently much more conservative, Fig. 6. These numerical model results obtained using the Goodall formula for calculation of the hoop stress in the pipe elbow are in good agreement with results reported by Duan and Shen [32] for the case when the maximum strain is located in the inner wall at the intrados of the pipe elbow.

Fig. 6. Comparison between the limit pressure values in the straight pipe (API 5L X52) and the pipe elbow (at the intrados section) for different depth ratios (d/t= 0.1 - 0.8) of the rectangular parallelepiped-shaped corrosion defects with rounded corners, obtained numerically by FEA, and analytically using standard (straight pipe) and modified (pipe elbow) codes.

Table 4 The difference in the limit pressure P_L values for the pipe elbow based on the ultimate strength (P_L •$_{ult(FEA)}$) obtained by FEA, and by modified codes (B31G, modified B31G, and DNV RP-F101) using the Goodall formula for calculation of the hoop stress in the pipe elbow.

3.3. The notch failure assessment diagram (NFAD) for the straight pipe and pipe bends with corrosion defects

In this final subsection, the notch failure assessment diagram (NFAD) for the straight pipe and pipe bends with corrosion defects is presented and analyzed. The assessment point in NFAD is defined with two non-dimensional parameters - coordinates (L_r, K_r), where L_r is applied stress (load), and K_r is a driving force. As mentioned in the introduction section, these two parameters - coordinates in the NFAD substitute three influencing parameters, the fracture toughness (K•$_C$), defect depth ratio *(d/t)*, and the internal pressure *(P)*. In this study, the NFAD was modified using the pipe elbow hoop stress •. in the equation for calculation of a non-dimensional load L_r according to the following equation L_r= •. /•., where •. and •. are the hoop stress (maximum circumferential stress), and flow stress, respectively [12]. The flow stress •. is expressed by the following equation •.= (•$_y$ +•$_{ult}$) / 2, where •$_y$ and •$_{ult}$ are the yield strength and ultimate strength, respectively [12,84]. The values of •$_y$ and •$_{ult}$ for API 5L X52 steel used in this study are shown in Table 2. Also, for the calculation of a non-dimensional crack driving force K_r in the pipe elbow, a maximum equivalent notch stress intensity factor (K•$_{eq}$) is used and computed because of the elbow curvature which provoked

the more complex mixed mode of loading ($K_{I\bullet}$, $K_{II\bullet}$, and $K_{III\bullet}$, $K_{\bullet eq}$= f ($K_{I\bullet}$, $K_{II\bullet}$, and $K_{III\bullet}$)) according to the following equation $K_r = K_{\bullet eq} / K_{\bullet C}$ [12]. Calculated fracture toughness values for the pipe elbow ($K_{\bullet C}$= 95 MPa.m$^{0.5}$) and straight pipe ($K_{\bullet C}$= 116.6 MPa.m$^{0.5}$) made of the same material (API 5L X52 steel), and with the same dimensions and geometry, are taken from our previous study (see Table 2) [12]. Also, the fracture toughness value for the pipe elbow is less than for the straight pipe due to a higher constraint [12]. The NFAD is based on the interpolation curve K_r= f (L_r) and it is typically presented in polar coordinates (r, $\bullet$) [84]. A schematic representation of a typical NFAD with two characteristic polar angle values ($\bullet_1$ and $\bullet_2$) that defined three typical domains ($\bullet > \bullet_1$ - brittle fracture, $\bullet_1 > \bullet > \bullet_2$ - elasto-plastic fracture, and $\bullet < \bullet_2$ - plastic collapse) is shown in Fig. 7. Failure happens if the assessment point (L_r, K_r) is above the interpolation - failure curve K_r= f (L_r) [84]. More details about polar angles definition, three typical domains, and the application of the NFAD are presented in numerous previously published works [12,39,41,64-75,84,86].

Figure 8 shows the NFAD for the straight pipe and pipe elbow with different depth ratios (d/t= 0.1 - 0.8) of the rectangular parallelepiped-shaped corrosion defects with rounded corners at the intrados section. Evolutions of the function point coordinates, which define the assessment point on the NFAD, indicate that the pipe elbow is a more endangered component of the pipeline. For all corrosion defect depth ratios, the assessment points for the pipe elbow have a higher value of both coordinates (L_r, K_r) than for the straight pipe due to the stress amplification and higher constraint in pipe elbows. Particularly, the non-dimensional applied crack driving force K_r coordinates for all corrosion defect depth ratios are higher for the pipe elbows. The difference between the K_r coordinate for the pipe elbow and straight pipe increases significantly with an increase of the corrosion defect depth ratio d/t from 0.1 to 0.8. Therefore, only at the lowest corrosion defect depth ratio (d/t= 0.1), the pipe elbow assessment point is in the elasto-plastic failure domain of the NFAD. A further significant rise of the K_r coordinates at somewhat higher d/t ratios ($0.1 < d/t \leq 0.38$), provokes conditions for the pipe elbow assessment points to be shifted into the brittle zone of the NFAD, but still within the safety zone. The loading path increases in a more non-linearly way with the rise of crack depth ratio d/t ($0.38 < d/t \leq 0.8$) at the intrados section of the pipe elbow. Also, for the corrosion depth ratios higher than the critical ($d/t > 0.38$), all assessment points are located in the failure zone of the NFAD, Fig. 8. The obtained critical depth ratio (d/t= 0.38) of the rectangular parallelepiped-shaped corrosion defect with rounded corners for the pipe elbow is

somewhat higher than the critical semi-elliptical relative crack depth ratio (d/t= 0.28) in the pipe elbow obtained in our previous study [12].

The loading path increases in a more linear way for the straight pipe with different corrosion defect depth ratio. More linear behavior is mainly the consequence of the lower increments of the corresponding K_r coordinates for the straight pipe with the increase of d/t. The obtained critical depth ratio (d/t= 0.69) of the rectangular parallelepiped-shaped corrosion defect with rounded corners for the straight pipe is significantly higher than for the pipe elbow (d/t= 0.38). Moreover, all assessment points for the straight pipe with corrosion defect depth ratios below the critical ($0.1 < d/t \leq 0.69$) are located in the least dangerous plastic collapse fracture domain of the NFAD, as shown in Fig. 8. The obtained critical depth ratio (d/t= 0.69) of the rectangular parallelepiped-shaped corrosion defect with rounded corners for the straight pipe, Fig. 8, is slightly higher than for the critical semi-elliptical relative crack depth ratio (d/t= 0.66) in the straight pipe obtained in our previous study [12]. Also, for the crack depth ratios lower than the critical ($0.1 < d/t \leq 0.66$), investigated in our previous study [12], all assessment points were located in the more dangerous elasto-plastic fracture domain of the NFAD. Contrary, in this study of the rectangular parallelepiped-shaped corrosion defects with rounded corners in the straight pipe, for all defect depth ratios lower than the critical ($0.1 < d/t \leq 0.69$), the assessment points are located in the less dangerous plastic collapse fracture domain of the NFAD, as shown in Fig. 8.

It can be concluded that due to more pronounced stress intensification provoked by the semi-elliptical cracks with different relative depth rations [12], the structural integrity and reliability of both straight pipe and pipe elbow is more threatened than in the case of a rectangular parallelepiped-shaped corrosion defect with rounded corners. The results presented in this study indicate further that the more severe stress conditions in pipe elbows with corrosion defect at the intrados section in comparison to the straight pipe lead to the shift of assessment points into the brittle zone of the modified NFAD. According to the codes, previously analyzed in subsection 3.2, the straight pipe can resist the defect depths which reach 80 - 85 % of pipe wall thickness [33,81,85]. The results presented in this study and the NFAD for the straight pipe indicate that such a criterion is overly optimistic and hence not universally applicable. The presented results are proving the applicability and practical benefits of the modified NFAD. The NFAD is useful for the reliability assessment of corroded pipes and particularly critical pipe elbows taking into account the different shapes and depth of defects and the significant stress intensification in pipe elbows.

Fig. 7. The schematic view of the notch failure assessment diagram (NFAD) and three typical domains. Adapted and modified from [84].

Fig. 8. Notch failure assessment diagram (NFAD) for the straight pipe and pipe elbow with different depth ratios (d/t= 0.1 - 0.8) of the rectangular parallelepiped-shaped corrosion defects with rounded corners at the intrados section.

4. Conclusions

A comprehensive study of safety and reliability assessment of the corroded pipe elbow and the straight pipe made of API 5L X52 pipeline steel using the numerical FEA, including the applicability of the modified codes adapted for the pipe elbow, is presented in this paper. Regarding the results of the limit pressure calculation and the hoop stress values in the pipe elbow with and without different rectangular parallelepiped-shaped corrosion defect depth ratios (d/t= 0.1 - 0.8) and the applicability of the modified codes using the Goodall formula for calculation of the hoop stress, the following conclusions can be drawn.

- There is a good agreement between the hoop stress value obtained using the Goodall formula for calculation of the hoop stress at the intrados section of a pipe elbow without corrosion defects and the value obtained by the FEA with the small error of 5.32 %.
- The much higher error (25.94 %) is obtained using the straight pipe formula for the calculation of the hoop stress in the pipe elbow.
- The results of the limit pressure calculations using the modified codes that take into account the pipe elbow geometry by using the Goodall formula for calculation of the hoop stress in the pipe elbow are in close agreement with the numerical FEA results.
- Both conservative trend and overestimation in the limit pressure values obtained using ASME B31G code with the highest errors (from 10.56 up to 17.93 %) of all three used models in comparison with the numerical FEA results for analyzed defect depth ratios (d/t= 0.1 - 0.8) are observed.

- The results for the limit pressure obtained using the other two modified standards (modified ASME B31G, and DNV RP-F101) are less conservative and in much better agreement with the numerical FEA results based on the ultimate strength.
- The results for the limit pressure obtained using the modified ASME B31G standard are closest to the numerical FEA results for all defect depth ratios (error: 2.49 - 10.27 %).
- The numerical FEA results for the limit pressure in the pipe elbow using the yield strength for different defect depth ratios are consistently much more conservative and hence not applicable in this study.

The results obtained in the previous research have proved the practical benefits of the modified notch failure assessment diagram (NFAD) for the assessment of the structural integrity and reliability of straight pipes and pipe elbows with different corrosion defects. Based on the comprehensive reliability analysis using the NFAD for the straight pipe and pipe bends (API 5L X52) with different depth ratios (d/t= 0.1 - 0.8) of the rectangular parallelepiped-shaped corrosion defect with rounded corners at the intrados section the following conclusions can be drawn.

- For the calculation of a non-dimensional crack driving force K_r in the pipe elbow, a maximum equivalent notch stress intensity factor ($K_{\bullet eq}$) should be computed and used since the elbow curvature provoked the complex mixed mode of loading. The obtained fracture toughness value for the pipe elbow is less than for the straight pipe due to a higher constraint.
- The assessment points for the pipe elbow have a higher value of both coordinates (L_r, K_r) for all corrosion defect depth ratios than for the straight pipe, due to the stress intensification and higher constrain in the pipe elbows.
- For the corrosion defect depth ratios higher than 0.2 (d/t> 0.2), the pipe elbow assessment points are located in the brittle zone of the NFAD, while the critical corrosion defect depth ratio (in the failure zone of the NFAD) is d/t= 0.38.
- The obtained critical corrosion defect depth ratio (d/t= 0.69) for the straight pipe is significantly higher than for the pipe elbow (d/t= 0.38). Also, all assessment points for corrosion defect depth ratios below the critical are located in the least dangerous plastic collapse fracture domain of the NFAD.

This study confirms that the pipe elbow is a critical part of piping systems. Moreover, the stresses at the intrados section of the pipe elbow are higher than at extrados or crown sections. Due to these facts, unmodified codes developed for the straight pipes are not applicable for pipe elbows. Further investigation of modified codes for the limit pressure calculation in the pipe elbow, taking into account the application of different contemporary formulas for the calculation of the hoop stress, is envisaged in our future research.

References

[1] Djukic, M.B., Zeravcic, V.S., Bakic, G.M., Sedmak. A. and Rajicic B., 2015. Hydrogen damage of steels: A case study and hydrogen embrittlement model. Engineering Failure Analysis, 58, pp.485-498, https://doi.org/10.1016/j.engfailanal.2015.05.017

[2] Popov, B.N., Lee, J.W., and Djukic, M.B., 2018. Hydrogen permeation and hydrogen-induced cracking. In Myer Kutz, editor. Handbook of Environmental Degradation of Materials, Third Edition. William Andrew Publishing, pp.133-162,

https://doi.org/10.1016/B978-0-323-52472-8.00007-1

[3] Wasim, M. and Djukic, M.B., 2020. Hydrogen embrittlement of low carbon structural steel at macro-, micro- and nano-levels. International Journal of Hydrogen Energy, 45(3), pp.2145-2156, https://doi.org/10.1016/j.ijhydene.2019.11.070

[4] Djukic, M.B., Bakic, G.M., Zeravcic, V.S., Sedmak, A. and Rajicic, B., 2019. The synergistic action and interplay of hydrogen embrittlement mechanisms in steels and iron: Localized plasticity and decohesion. Engineering Fracture Mechanics, 216, p.106528, https://doi.org/10.1016/j.engfracmech.2019.106528

[5] Wasim, M. and Djukic, M.B., 2020. Long-term external microbiologically influenced corrosion of buried cast iron pipes in the presence of sulfate-reducing bacteria (SRB). Engineering Failure Analysis, 115, p.104657,

https://doi.org/10.1016/j.engfailanal.2020.104657

[6] Bakic, G.M., Djukic, M.B., Rajicic, B., Zeravcic, V.S., Maslarevic, A. and Milosevic, N., 2016. Oxidation behavior during prolonged service of boiler tubes made of 2.25Cr1Mo and 12Cr1Mo0.3V heat resistance steels. Procedia Structural Integrity, 2, pp.3647-3653, https://doi.org/10.1016/j.prostr.2016.06.453

[7] Baki□, G.M., Šija□kiŽerav□i□, V.M., Djuki□, M.B., Maksimovi□, S.M., Plešinac, D.S. and Raji□i□, B.M., 2011. Thermal history and stress state of a fresh steam-pipeline influencing its remaining service life. Thermal Science, 15(3), pp.691-704,

https://doi.org/10.2298/TSCI110509050B

[8] Meriem-Benziane, M., Bou-Saïd, B. and Boudouani, N., 2017. The effect of crude oil in the pipeline corrosion by the naphthenic acid and the sulfur: A numerical approach. Journal of Petroleum Science and Engineering, 158, pp.672-679,

https://doi.org/10.1016/j.petrol.2017.08.073

[9] Soudani, M., Bouledroua, O., Hadj Meliani, M., El-Miloudi, K., Muthanna, B.G.N., Khelil, A., Elhoud, A., Matvienko, Y.G. and Pluvinage, G., 2018. Corrosion inspection and recommendation on the internal wall degradation caused rupture of 6" gas line pipe. Journal of Bio-and Tribo-Corrosion, 4(2), p.28, https://doi.org/10.1007/s40735-018-0145-0

[10] Amara, M., Bouledroua, O., Hadj Meliani, M., Muthanna, B.G.N., Tahar Abbes, M. and Pluvinage, G., 2018. Assessment of pipe for CO_2 transportation using a constraint modified ctod failure assessment diagram. Structural Integrity and Life, 18(2), pp.149-153,

http://divk.inovacionicentar.rs/ivk/ivk18/149-IVK2-2018-MA-OB-MHM-BGNM-MTA-GP.pdf

[11] Yu, W., Fede, P., Climent, E. and Sanders, S., 2019. Multi-fluid approach for the numerical prediction of wall erosion in an elbow. Powder Technology, 354, pp.561-583, https://doi.org/10.1016/j.powtec.2019.06.007

[12] Muthanna, B.G.N., Bouledroua, O., Meriem-Benziane, M., Hadj Meliani, M., Pluvinage, G. and Suleiman, R.K., 2019. Numerical study of semi-elliptical cracks in the critical position of pipe elbow. Frattura ed Integrità Strutturale, 13(49), pp.463-477,

https://doi.org/10.3221/IGF-ESIS.49.44

[13] Peng, W., Cao, X., Hou, J., Xu, K., Fan, Y. and Xing, S., 2020. Experiment and numerical simulation of sand particle erosion under slug flow condition in a horizontal pipe bend. Journal of Natural Gas Science and Engineering, 76, p.103175,

https://doi.org/10.1016/j.jngse.2020.103175

[14] Amara, M., Muthanna, B.G.N., Tahar Abbes, M. and Hadj Meliani, M., 2018. Effect of sand particles on the Erosion-corrosion for a different locations of carbon steel pipe elbow. Procedia Structural Integrity, 13, pp.2137-2142,

https://doi.org/10.1016/j.prostr.2018.12.151

[15] Tawancy, H.M., Al-Hadhrami, L.M. and Al-Yousef, F.K., 2013. Analysis of corroded elbow section of carbon steel piping system of an oil–gas separator vessel. Case Studies in Engineering Failure Analysis, 1(1), pp.6-14,

https://doi.org/10.1016/j.csefa.2012.11.001

[16] Muthanna, B.G.N., Amara, M., Hadj Meliani, M., Mettai, B., Boži□, Ž., Suleiman, R. and Sorour, A.A., 2019. Inspection of internal erosion-corrosion of elbow pipe in the desalination station. Engineering Failure Analysis, 102, pp.293-302, https://doi.org/10.1016/j.engfailanal.2019.04.062

[17] Kusmono and Khasani, 2017. Analysis of a failed pipe elbow in geothermal production facility. Case Studies in Engineering Failure Analysis, 9, pp. 71-77,

https://doi.org/10.1016/j.csefa.2017.08.001

[18] Qiao, Q., Cheng, G., Li, Y., Wu, W., Hu, H. and Huang, H., 2017. Corrosion failure analyses of an elbow and an elbow-to-pipe weld in a natural gas gathering pipeline. Engineering Failure Analysis, 82, pp. 599-616,

https://doi.org/10.1016/j.engfailanal.2017.04.016

[19] Ilman, M.N., 2014. Analysis of internal corrosion in subsea oil pipeline. case studies in Engineering Failure Analysis, 2(1), pp.1-8, https://doi.org/10.1016/j.csefa.2013.12.003

[20] Li, L., Li, C.Q. and Mahmoodian, M., 2019. Prediction of fatigue failure of steel beams subjected to simultaneous corrosion and cyclic loading. Structures, 19, pp. 386-393, https://doi.org/10.1016/j.istruc.2019.02.003

[21] Kim, J.W., Na, Y.S. and Lee, S.H., 2009. Experimental evaluation of the bending load effect on the failure pressure of wall-thinned elbows. Journal of Pressure Vessel Technology, 131(3), p.031210, https://doi.org/10.1115/1.3122032

[22] Li, Y., Zhao, J.H., Zhu, Q. and Cao, X.Y., 2015. Unified Solution of Burst Pressure for Defect-Free Thin Walled Elbows. Journal of Pressure Vessel Technology, 137(2), p.021203, https://doi.org/10.1115/1.4028068

[23] Xie, Y.J., Zhang, H., Liu, S., Yang, P. and Luo, X., 2013. A Study on Stress Corrosion Crack of Thick-Walled Elbow in Manifold for Acid Fracturing. Journal of Pressure Vessel Technology, 135(2), p.021207, https://doi.org/10.1115/1.4023420

[24] Zhang, S.H., Gao, C.R., Zhao, D.W. and Wang, G.D., 2013. Limit analysis of defect-free pipe elbow under internal pressure with mean yield criterion. Journal of Iron and Steel Research, International, 20(4), pp.11-15, https://doi.org/10.1016/S1006-706X(13)60075-8

[25] Li, Z., Yinpei, W., Jin, C. and Cengdian, L., 2001. Evaluation of local thinned pressurized elbows. International Journal of Pressure Vessels and Piping, 78(10), pp.697-703, https://doi.org/10.1016/S0308-0161(01)00125-9

[26] Lee, G.H., Seo, J.K. and Paik, J.K., 2017. Condition assessment of damaged elbow in subsea pipelines. Ships and Offshore Structures, 12(1), pp.135-151,

https://doi.org/10.1080/17445302.2015.1116245

[27] Kim, Y.J. and Oh, C.S., 2006. Limit loads for pipe bends under combined pressure and in-plane bending based on finite element limit analysis. International Journal of Pressure Vessels and Piping, 83(2), pp.148-153, https://doi.org/10.1016/j.ijpvp.2005.11.001

[28] Khalajestani, M.K., Bahaari, M.R., Salehi, A. and Shahbazi, S., 2015. Predicting the limit pressure capacity of pipe elbows containing single defects. Applied Ocean Research, 53, pp.15-22, https://doi.org/10.1016/j.apor.2015.07.002

[29] Khalajestani, M.K. and Bahaari, M.R., 2014. Investigation of pressurized elbows containing interacting corrosion defects. International Journal of Pressure Vessels and Piping, 123, pp.77-85, https://doi.org/10.1016/j.ijpvp.2014.08.002

[30] Hong, S.P., Kim, J.H. and Kim, Y.J., 2009. Limit pressures of 90 elbows with circumferential surface cracks. Engineering Fracture Mechanics, 76(14), pp.2202-2216, https://doi.org/10.1016/j.engfracmech.2009.07.005

[31] Chattopadhyay, J. and Tomar, A.K.S., 2006. New plastic collapse moment equations of defect-free and throughwall circumferentially cracked elbows subjected to combined internal pressure and in-plane bending moment. Engineering Fracture Mechanics, 73(7), pp.829-854, https://doi.org/10.1016/j.engfracmech.2005.12.002

[32] Duan, Z.X. and Shen, S.M., 2006. Analysis and experiments on the plastic limit pressure of elbows. International journal of pressure vessels and piping, 83(10), pp.707-713, https://doi.org/10.1016/j.ijpvp.2006.08.003

[33] Lee, G.H., Pouraria, H., Seo, J.K. and Paik, J.K., 2015. Burst strength behaviour of an aging subsea gas pipeline elbow in different external and internal corrosion-damaged

positions. International Journal of Naval Architecture and Ocean Engineering, 7(3), pp.435-451, https://doi.org/10.1515/ijnaoe-2015-0031

[34] Mahdi, R.S. and Zahiraniza, M., 2019. Rehabilitation of Corroded Circular Hollow Sectional Steel Beam by CFRP Patch. Steel and Composite Structures, 32(1), pp.127-139, https://doi.org/10.12989/scs.2019.32.1.127

[35] Mahdi, R.S., Zahiraniza, M., Biramarta, I., Nasir, S., Zubair I.S. and Do Kyan, K., 2016 Meso-Scale Numerical Study of Composite Patch Repaired Hole Drilled Steel Plate. ARPN Journal of Engineering and Applied Sciences, 11(3), pp.1724-1728,

http://www.arpnjournals.org/jeas/research_papers/rp_2016/jeas_0216_3557.pdf

[36] Mahdi R.S., Zahiraniza M., Nasir S., BiramartaI. and ZubairI. S., Finite Element Modeling of Wet Lay-up CFRP Patch Repaired Corroded Offshore Steel Jacket Member. Offshore Technology Conference (OTC) Asia, Malaysia, 2016,

https://doi.org/10.4043/26737-MS

[37] Firoozabad, E.S., Jeon, B.G., Choi, H.S. and Kim, N.S., 2016. Failure criterion for steel pipe elbows under cyclic loading. Engineering Failure Analysis, 66, pp.515-525, https://doi.org/10.1016/j.engfailanal.2016.05.012

[38] Zelmati, D., Ghelloudj, O. and Amirat, A., 2017. Reliability estimation of pressurized API 5L X70 pipeline steel under longitudinal elliptical corrosion defect. The International Journal of Advanced Manufacturing Technology, 90(9-12), pp.2777-2783,

https://doi.org/10.1007/s00170-016-9580-6

[39] Zelmati, D., Ghelloudj, O. and Amirat, A., 2017. Correlation between defect depth and defect length through a reliability index when evaluating of the remaining life of steel pipeline under corrosion and crack defects. Engineering Failure Analysis, 79, pp.171-185, https://doi.org/10.1016/j.engfailanal.2017.04.025

[40] Zhou, W., 2010. System reliability of corroding pipelines. International Journal of Pressure Vessels and Piping, 87(10), pp.587-595, https://doi.org/10.1016/j.ijpvp.2010.07.011

[41] Bouledroua, O., Zelmati, D. and Hassani, M., 2019. Inspections, statistical and reliability assessment study of corroded pipeline. Engineering failure analysis, 100, pp.1-10, https://doi.org/10.1016/j.engfailanal.2019.02.012

[42] Maxey, W.A., Kiefner, J.F., Eiber, R.J. and Duffy, A.R., 1972. Ductile fracture initiation, propagation, and arrest in cylindrical vessels. In Fracture Toughness: Part II, ed. H. Corten (West Conshohocken, PA: ASTM International, 1972), pp.70-81,

https://doi.org/10.1520/STP38819S

[43] ASME, Manual for Determining the Remaining Strength of Corroded Pipelines- a Supplement to ASME B31 Code for Pressure Piping, The American Society of Mechanical Engineers, New York, 1991.

[44] Kiefner, J. and Vieth, P., A Modified Criterion for Evaluating the Remaining Strength of Corroded Pipe, Final Report on Project PR 3-805, Battelle Memorial Institute, Columbus, OH, 1989, 1989.

[45] DNV Recommended Practice, RP-F101. Corroded pipelines. Det Norske Veritas; 2004

[46] Ritchie, D. and Last, S., 1995, April. Burst criteria of corroded pipelines-defect acceptance criteria. In Proceedings of the EPRG/PRC 10th biennial joint technical meeting on line pipe research.

[47] Kiefner, J.F. and Vieth, P.H., PC program speeds new criterion for evaluating corroded pipe, Oil Gas J. (1990) 91–93. August 20, 1990.

[48] Stephens, D.R. and Leis, B.N., Development of an alternative criterion for residual strength of corrosion defects in moderate-to high-toughness pipe, In: 2000 3rd International Pipeline Conference, October 1–5, 2000, Calgary, Alberta, Canada American Society of Mechanical Engineers, 2000, p.IPC2000-192, https://doi.org/10.1115/IPC2000-192

[49] Wang, Q. and Zhou, W., 2019. A new burst pressure model for thin-walled pipe elbows containing metal-loss corrosion defects. Engineering Structures, 200, p.109720, https://doi.org/10.1016/j.engstruct.2019.109720

[50] Yahiaoui, K., Moffat, D.G. and Moreton, D.N., 2000. Piping elbows with cracks Part 2: global finite element and experimental plastic loads under opening bending. The Journal of Strain Analysis for Engineering Design, 35(1), pp.47-57,

https://doi.org/10.1243/0309324001514008

[51] Goodall, I.W., 1978. Lower bound limit analysis of curved tubes loaded by combined internal pressure and in-plane bending moment. Research Division Report RD/B N, 4360, p.14.

[52] Kim, J.W., Yoon, M.S. and Park, C.Y., 2013. The effect of load-controlled bending load on the failure pressure of wall-thinned pipe elbows. Nuclear Engineering and Design, 265, pp.174-183, https://doi.org/10.1016/j.nucengdes.2013.07.027

[53] Tee, K.F. and Wordu, A.H., 2020. Burst strength analysis of pressurized steel pipelines with corrosion and gouge defects. Engineering Failure Analysis, 108, p.104347, https://doi.org/10.1016/j.engfailanal.2019.104347

[54] Yang, S., Li, C.Q. and Yang, W., 2016. Analytical model of elastic fracture toughness for steel pipes with internal cracks. Engineering Fracture Mechanics, 153, pp.50-60, https://doi.org/10.1016/j.engfracmech.2015.11.014

[55] Pluvinage, G., 1998. Fatigue and fracture emanating from notch; the use of the notch stress intensity factor. Nuclear Engineering and Design, 185(2-3), pp.173-184, https://doi.org/10.1016/S0029-5493(98)00183-6

[56] Adib, H., Jallouf, S., Schmitt, C., Carmasol, A. and Pluvinage, G., 2007. Evaluation of the effect of corrosion defects on the structural integrity of X52 gas pipelines using the SINTAP procedure and notch theory. International journal of pressure vessels and piping, 84(3), pp.123-131, https://doi.org/10.1016/j.ijpvp.2006.10.005

[57] Hadj Meliani, M., Pluvinage, G. and Capelle, J., 2009. Gouge assessment for pipes and associated transferability problem. In Defect and Diffusion Forum (Vol. 294, pp.15-25). Trans Tech Publications Ltd, https://doi.org/10.1016/j.engfailanal.2010.01.007

[58] Pluvinage, G., Capelle, J. and Hadj Meliani, M., 2019. Pipe networks transporting hydrogen pure or blended with natural gas, design and maintenance. Engineering Failure Analysis, 106, pp.104-164, https://doi.org/10.1016/j.engfailanal.2019.104164

[59] Hadj Meliani, M., Azari, Z., Pluvinage, G. and Capelle, J., 2010. Gouge assessment for pipes and associated transferability problem. Engineering Failure Analysis, 5(17), pp.1117-1126, https://doi.org/10.1016/j.engfailanal.2010.01.007

[60] Moustabchir, H., Zitouni, A., Hariri, S., Gilgert, J. and Pruncu, C.I., 2018. Experimental–numerical characterization of the fracture behaviour of P264GH steel notched pipes subject to internal pressure. Iranian Journal of Science and Technology, Transactions of Mechanical Engineering, 42(2), pp.107-115, https://doi.org/10.1007/s40997-017-0086-0

[61] Adib, H. and Pluvinage, G., 2003. Theoretical and numerical aspects of the volumetric approach for fatigue life prediction in notched components. International Journal of fatigue, 25(1), pp.67-76, https://doi.org/10.1016/S0142-1123(02)00040-3

[62] Adib-Ramezani, H., Jeong, J. and Pluvinage, G., 2006. Structural integrity evaluation of X52 gas pipes subjected to external corrosion defects using the SINTAP procedure. International Journal of Pressure Vessels and Piping, 83(6), pp.420-432, https://doi.org/10.1016/j.ijpvp.2006.02.023

[63] Chattopadhyay, J., Pavankumar, T.V., Dutta, B.K. and Kushwaha, H.S., 2005. Fracture experiments on through wall cracked elbows under in-plane bending moment: Test results and theoretical/numerical analyses. Engineering fracture mechanics, 72(10), pp.1461-1497, https://doi.org/10.1016/j.engfracmech.2004.11.005

[64] Ainsworth, R.A., Gintalas, M., Sahu, M.K., Chattopadhyay, J. and Dutta, B.K., 2016. Application of failure assessment diagram methods to cracked straight pipes and elbows. International Journal of Pressure Vessels and Piping, 148, pp.26-35, https://doi.org/10.1016/j.ijpvp.2016.10.005

[65] Ainsworth, R.A., Gintalas, M., Sahu, M.K., Chattopadhyay, J. and Dutta, B.K., 2015. Failure Assessment Diagram Assessments of Large-Scale Cracked Straight Pipes and Elbows. Transactions, SMiRT-23 Manchester, United Kingdom - August 10-14, 2015.

http://www.lib.ncsu.edu/resolver/1840.20/33859

[66] Bouledroua, O., Hafsi, Z., Djukic, M.B. and Elaoud, S., 2020. The synergistic effects of hydrogen embrittlement and transient gas flow conditions on integrity assessment of a precracked steel pipeline. International Journal of Hydrogen Energy, https://doi.org/10.1016/j.ijhydene.2020.04.262

[67] Boukortt, H., Amara, M., Hadj Meliani, M., Bouledroua, O., Muthanna, B.G.N., Suleiman, R.K., Sorour, A.A. and Pluvinage, G., 2018. Hydrogen embrittlement effect on the

structural integrity of API 5L X52 steel pipeline. International Journal of Hydrogen Energy, 43(42), pp.19615-19624, https://doi.org/10.1016/j.ijhydene.2018.08.149

[68] Meriem-Benziane, M., Abdul-Wahab, S.A., Zahloul, H., Babaziane, B., Hadj-Meliani, M. and Pluvinage, G., 2015. Finite element analysis of the integrity of an API X65 pipeline with a longitudinal crack repaired with single-and double-bonded composites. Composites Part B: Engineering, 77, pp.431-439, https://doi.org/10.1016/j.compositesb.2015.03.008

[69] Bouledroua, O., Hadj Meliani, M. and Pluvinage, G., 2017. Assessment of pipe defects using a constraint-modified failure assessment diagram. Journal of Failure Analysis and Prevention, 17(1), pp.144-153, https://doi.org/10.1007/s11668-016-0221-z

[70] Pluvinage, G., Bouledroua, O., Hadj Meliani, M. and Suleiman, R., 2018. Corrosion defect analysis using domain failure assessment diagram. International Journal of Pressure Vessels and Piping, 165, pp.126-134, https://doi.org/10.1016/j.ijpvp.2018.06.005

[71] Zhang, F., Rosenfeld, M. and Gustafson, J., 2018. Fitness for Service Analysis of the Circumferential Extent of Corrosion in Pipelines. In 2018 12th International Pipeline Conference. American Society of Mechanical Engineers, p.IPC2018-78338, V001T03A030, https://doi.org/10.1115/IPC2018-78338

[72] Amara, M., Bouledroua, O., Hadj Meliani, M., Azari, Z., Abbess, M.T., Pluvinage, G. and Bozic, Z., 2019. Effect of corrosion damage on a pipeline burst pressure and repairing methods. Archive of Applied Mechanics, 89(5), pp.939-951, https://doi.org/10.1007/s00419-019-01518-z

[73] Larrosa, N.O., Ainsworth, R.A., Akid, R., Budden, P.J., Davies, C.M., Hadley, I., Tice, D.R., Turnbull, A. and Zhou, S., 2017. 'Mind the gap'in fitness-for-service assessment procedures-review and summary of a recent workshop. International Journal of Pressure Vessels and Piping, 158, pp.1-19, https://doi.org/10.1016/j.ijpvp.2017.09.004

[74] Pluvinage, G., Bouledroua, O. and Meliani, M.H., 2018. Corrosion defect harmfulness by domain failure assessment diagram. Pipeline Science and Technology, 2(3), pp.163-177, https://doi.org/10.28999/2514-541X-2018-2-3-163-177

[75] Cosham, A., Hopkins, P. and Macdonald, K.A., 2007. Best practice for the assessment of defects in pipelines–Corrosion. Engineering Failure Analysis, 14(7), pp.1245-1265,

https://doi.org/10.1016/j.engfailanal.2006.11.035

[76] Zelmati, D., Bouledroua, O., Hafsi, Z. and Djukic, M.B., 2020. Probabilistic analysis of corroded pipeline under localized corrosion defects based on the intelligent inspection tool. Engineering Failure Analysis, 115, p.104683,

https://doi.org/10.1016/j.engfailanal.2020.104683

[77] Escoe, A.K., 2006. Piping and Pipelines Assessment Guide. Gulf Professional Publishing, Burlington, MA, https://doi.org/10.1016/B978-0-7506-7880-3.X5000-4

[78] BjØrnØy, O.H. and Marley, M.J., 2001. Assessment of corroded pipelines: past, present and future. In The Eleventh International Offshore and Polar Engineering Conference, 17-22 June, Stavanger, Norway. https://www.onepetro.org/conference-paper/ISOPE-I-01-138

[79] Stephens, D.R. and Francini, R.B., 2000. A review and evaluation of remaining strength criteria for corrosion defects in transmission pipelines. In Proceedings of ETCE/OMAE 2000 Joint Conference on Energy for the New Millennium, New Orleans, LA, USA (pp. 14-17).

[80] Zhang, S.H., Gao, C.R., Zhao, D.W. and Wang, G.D., 2013. Limit analysis of defect-free pipe elbow under internal pressure with mean yield criterion. Journal of Iron and Steel Research, International, 20(4), pp.11-15, https://doi.org/10.1016/S1006-706X(13)60075-8

[81] Miller, A.G., 1988. Review of limit loads of structures containing defects. International Journal of Pressure Vessels and Piping, 32(1-4), pp.197-327, https://doi.org/10.1016/0308-0161(88)90073-7

[82] Ansys® Academic Research Mechanical, Release 19.1

[83] Amandi, K.U., Diemuodeke, E.O. and Briggs T.A., 2019. Model for remaining strength estimation of a corroded pipeline with interacting defects for oil and gas operations. Cogent Engineering, 6(1), p.1663682, https://doi.org/10.1080/23311916.2019.1663682

[84] Hadj Meliani, M., Matvienko, Y.G., Pluvinage, G., 2011. Corrosion defect assessment on pipes using limit analysis and notch fracture mechanics. Engineering Failure Analysis, 18(1), pp.271-283, https://doi.org/10.1016/j.engfailanal.2010.09.006

[85] Amaya-Gómezac, R., Sánchez-Silva, M., Bastidas-Arteaga, M., Schoefs, F. and Muñoza, F., 2019. Reliability assessments of corroded pipelines based on internal pressure – A review. Engineering Failure Analysis, 98, pp.190-214,

https://doi.org/10.1016/j.engfailanal.2019.01.064

[86] Zareei, A. and Nabavi, S.M., 2016. Weight function for circumferential semi-elliptical cracks in cylinders due to residual stress fields induced by welding. Archive of Applied Mechanics, 86(7), pp.1219-1230, https://doi.org/10.1007/s00419-015-1087-3

LIST OF TABLES

Table 1 Codes for calculating limit pressure P_L of the straight pipe.

Code	Limit pressure, P_L	Strength reduction factor, $f(d/t)$	Folias Factor, M	Geometrical conditions
ASME B31G [43]	$\left(\frac{2\left(1.1\sigma_y\right)t}{D}\right)f\left(\frac{d}{t}\right)$	$\frac{1-(2/3)\cdot(d/t)}{1-(2/3)\cdot(d/t)/M}$	$\left(1+0.8\cdot\frac{L^2}{Dt}\right)^{0.5}$	$\left(0.8\cdot\frac{L^2}{Dt}\right)^{0.5}\cdot 4$
		$1-\frac{d}{t}$	-	$\left(0.8\cdot\frac{L^2}{Dt}\right)^{0.5}>4$
Modified ASME B31G [44]	$\left(\frac{2\left(1.1\sigma_y+69\right)t}{D}\right)f\left(\frac{d}{t}\right)$	$\frac{1-0.85\cdot(d/t)}{1-0.85\cdot(d/t)/M}$	$\left(1+0.6275\cdot\frac{L^2}{Dt}-0.003375\cdot\left(\frac{L^2}{Dt}\right)^2\right)^{0.5}$	$\left(\frac{L^2}{Dt}\right)\cdot 50$
		$\frac{1-0.85\cdot(d/t)}{1-0.85\cdot(d/t)/M}$	$\left(1+0.31\frac{L^2}{Dt}\right)^{0.5}$	$\left(\frac{L^2}{Dt}\right)>50$
DNV RP-F101 [45]	$\left(\frac{2\left(\sigma_{ult}\right)t}{D-t}\right)f\left(\frac{d}{t}\right)$	$\frac{1-(d/t)}{1-(d/t)/M}$	$\left(1+0.31\frac{L^2}{Dt}\right)^{0.5}$	
Shell-92 [46]	$\frac{1.8\sigma_{ult}t}{D}.f\left(\frac{d}{t}\right)$	$\frac{1-(d/t)}{1-(d/t)/M}$	$\left(1+0.8\frac{L^2}{Dt}\right)^{0.5}$	
RSTRENG [47]	$\frac{2\sigma_{ult}t}{D}.f\left(\frac{d}{t}\right)$	$1-(d/t)/M$	$\left(1+0.6275\cdot\frac{L^2}{Dt}-0.003375\cdot\left(\frac{L^2}{Dt}\right)^2\right)^{0.5}$	
PCORRC [48]	$\frac{2\sigma_{ult}t}{D}.f\left(\frac{d}{t}\right)$	$1-(d/t)*M$	$1-\exp\left(-0.157\frac{L}{\sqrt{D(t-d)/2}}\right)$	

Table 2 Mechanical properties of API 5L X52 pipeline steel.

Yield strength, σ_y (MPa)	Ultimate strength, σ_{ult} (MPa)	Elongation, A (%)	Fracture toughness, K_{IC} (MPa.m$^{0.5}$)
410	528	32	straight pipe: 116.6 [12] pipe elbow: 95 [12]

Table 3 Hoop stress σ_θ at the intrados section of the pipe elbow without corrosion defects.

Method of calculation	Hoop stress, σ_θ (MPa)	Error (%) = $(\sigma_{\theta\,(FEA)} - \sigma_{\theta\,(Eq.1,\,2)}) / \sigma_{\theta\,(FEA)}$ x 100 %
Numerical FEA model (Fig. 3)	$\sigma_{\theta\,(FEA)}$ = 212.69	-
Goodall formula [51] (Eq. (2))	$\sigma_{\theta\,(Eq.2)}$ = 201.39	5.32
Straight pipe formula (Eq. (1))	$\sigma_{\theta\,(Eq.1)}$ = 157.50	25.94

Table 4 The difference in the limit pressure P_L values for the pipe elbow based on the ultimate strength (P_L • $_{ult(FEA)}$) obtained by FEA, and by modified codes (B31G, modified B31G, and DNV RP-F101) using the Goodall formula for calculation of the hoop stress in the pipe elbow.

Defect depth ratio, *d/t*	P_L (MPa), see Fig. 6, and Error (%) = ($P_{L\ (B31G,\ Mod.\ B31G,\ and\ DNV)}$ - P_L • $_{ult(FEA)}$) / P_L • $_{ult(FEA)}$ x 100 %						
	P_L • $_{ult(FEA)}$ (MPa)	$P_{L\ (B31G)}$ (MPa)	Error (%)	$P_{L\ (Mod.\ B31G)}$ (MPa)	Error (%)	$P_{L\ (DNV)}$ (MPa)	Error (%)
0.1	16.19	14.48	10.56	16.59	2.49	17.32	6.95
0.2	15.37	13.91	9.48	15.81	2.86	16.58	7.87
0.3	14.45	13.31	7.91	14.94	3.41	15.72	8.79
0.4	13.35	12.65	5.21	13.98	4.72	14.70	10.14
0.5	12.12	11.95	1.40	12.90	6.45	13.48	11.25
0.6	10.72	11.19	4.39	11.69	9.03	11.99	11.85
0.7	9.35	10.37	10.87	10.31	10.27	10.12	8.26
0.8	8.03	9.47	17.93	8.73	8.77	7.72	3.89

LIST OF FIGURES

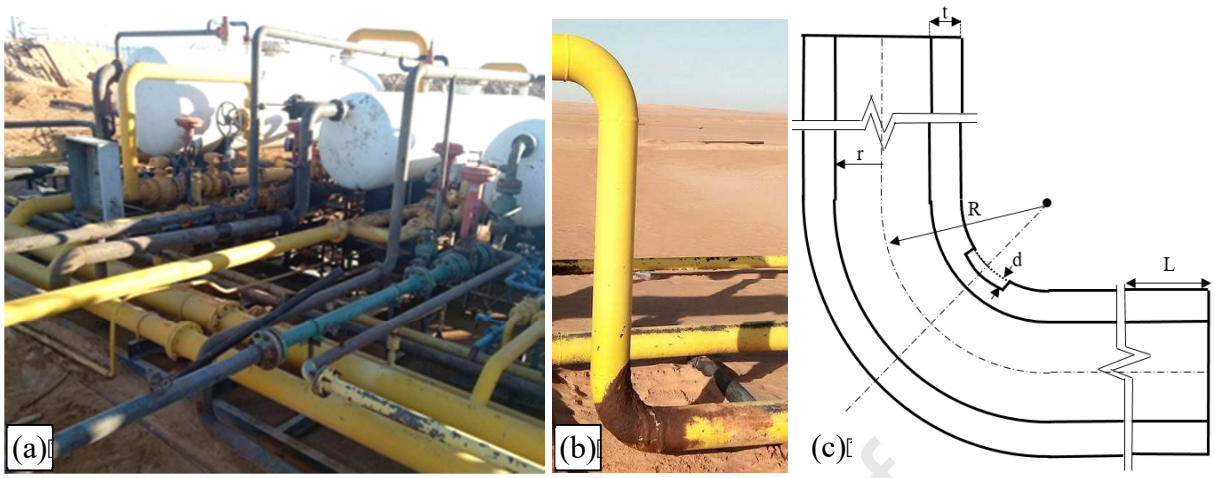

Fig. 1. API X52 pipeline elbow: (a) manifold separation system; (b) corroded pipe elbow; (c) pipe elbow dimensions.

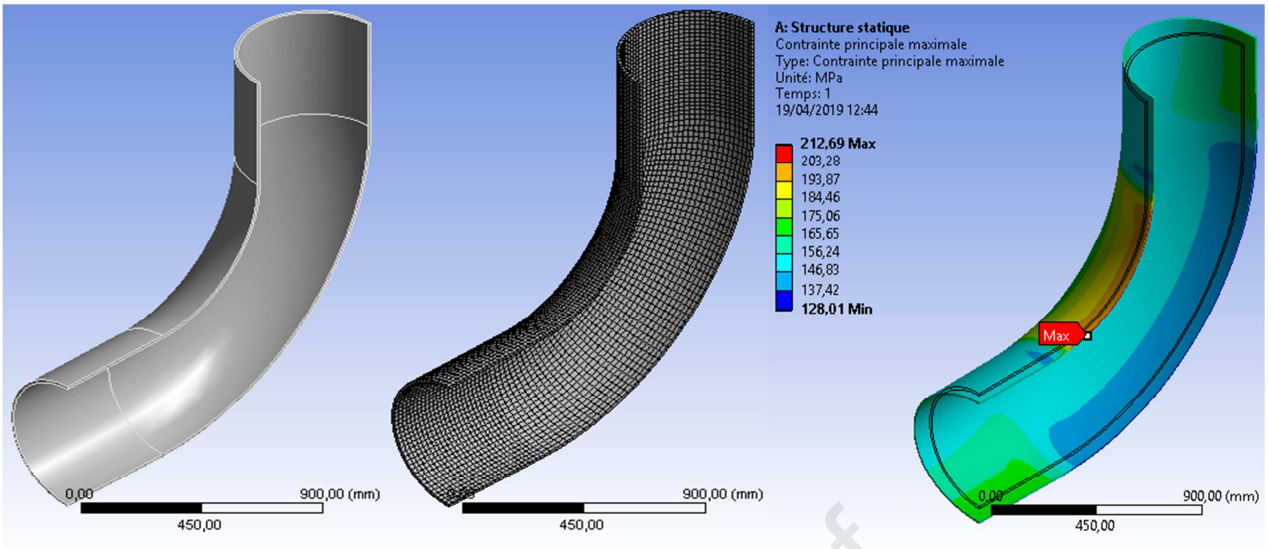

Fig. 2. Pipe elbow without corrosion defects subjected to the internal - service pressure P_s = 7 MPa, geometry, meshing, and hoop stress distribution.

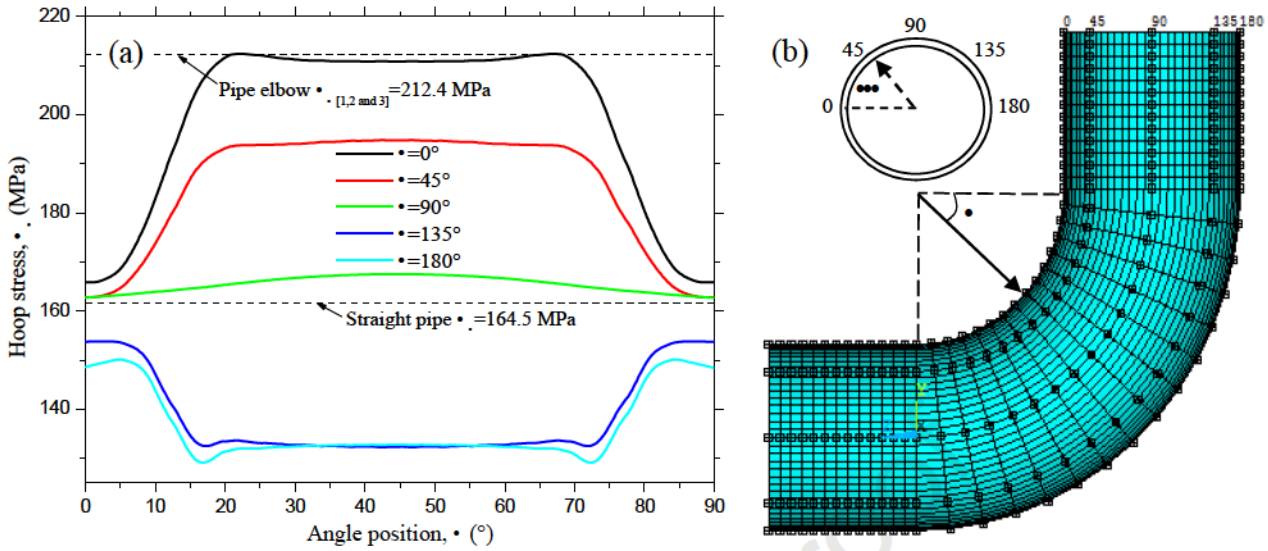

Fig. 3. Pipe elbow without corrosion defects: (a) distribution of the hoop stress; (b) different paths angles along the pipe elbow.

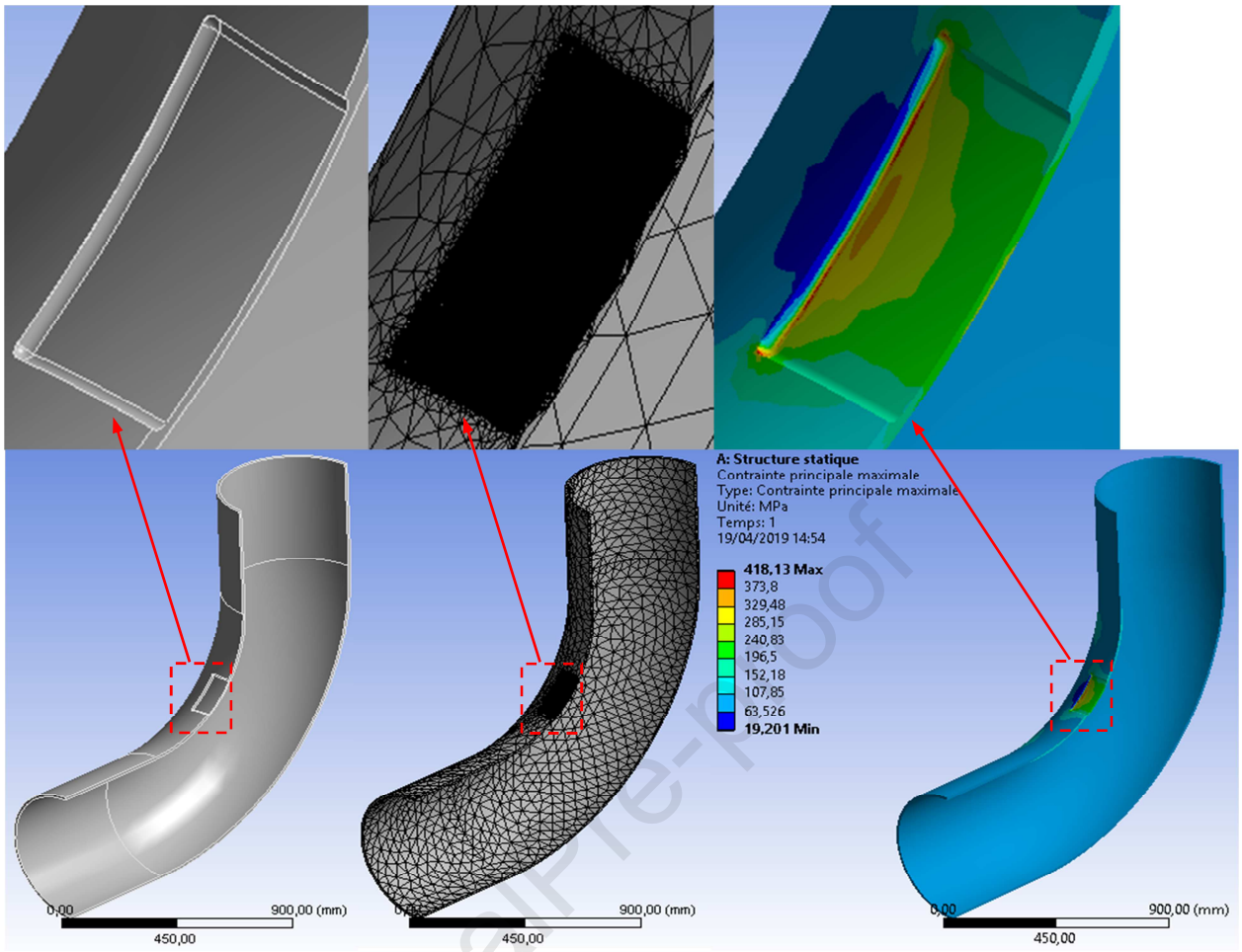

Fig. 4. Pipe elbow with rectangular parallelepiped-shaped corrosion defect with rounded corners at the intrados section subjected to the internal - service pressure P_s= 7 MPa: pipe elbow and the geometry of rectangular parallelepiped-shaped corrosion defect with rounded corners, meshing, and hoop stress distribution (d/t= 0.5).

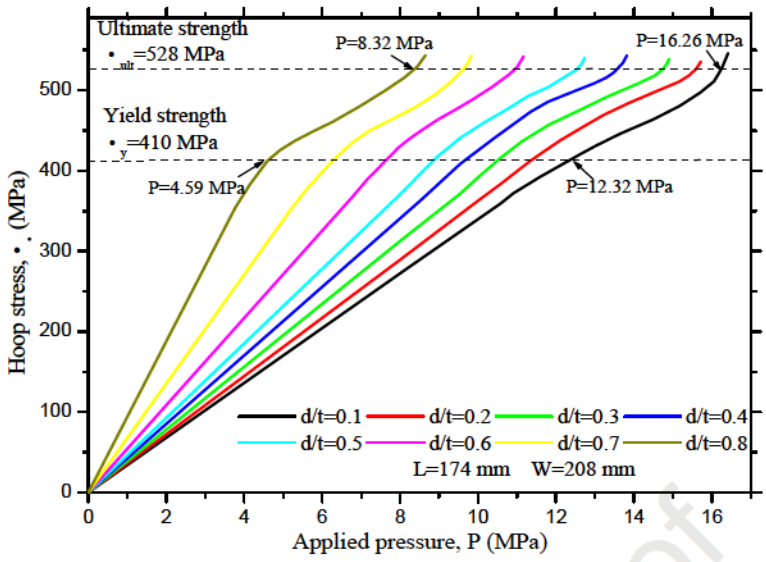

(a)

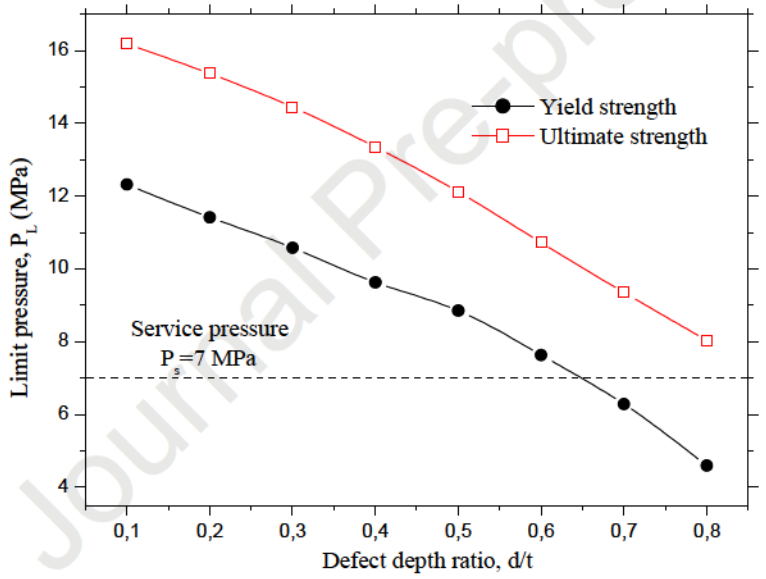

(b)

Fig. 5. Numerical analysis of elbow defects with different depth ratios *d/t* at the intrados section: (a) hoop stress versus internal pressure; (b) limit pressure P_L according to the yield and ultimate strength.

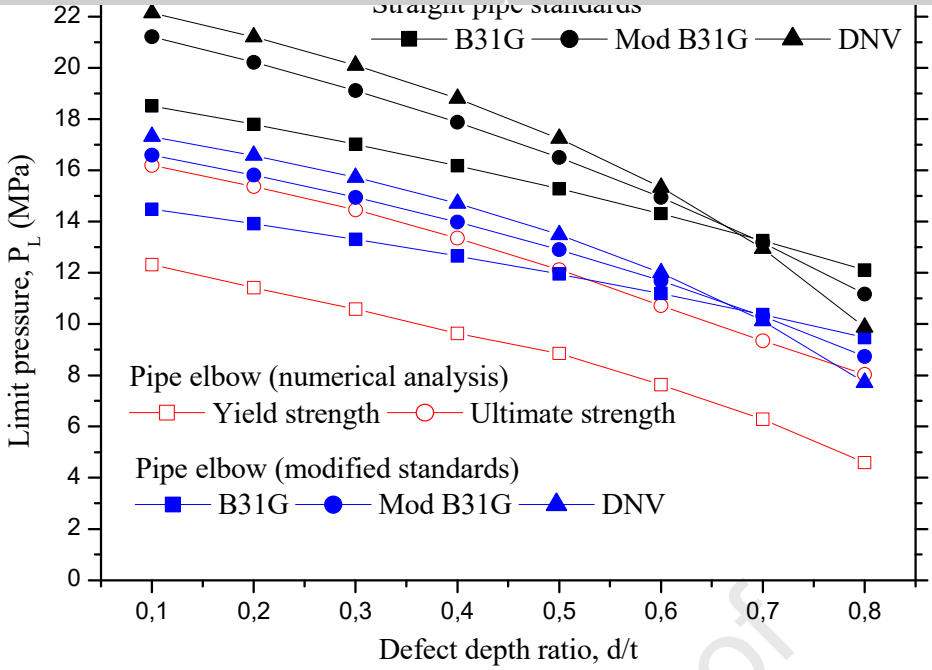

Fig. 6. Comparison between the limit pressure values in the straight pipe (API 5L X52) and the pipe elbow (at the intrados section) for different depth ratios (*d/t*= 0.1 - 0.8) of the rectangular parallelepiped-shaped corrosion defects with rounded corners, obtained numerically by FEA, and analytically using standard (straight pipe) and modified (pipe elbow) codes.

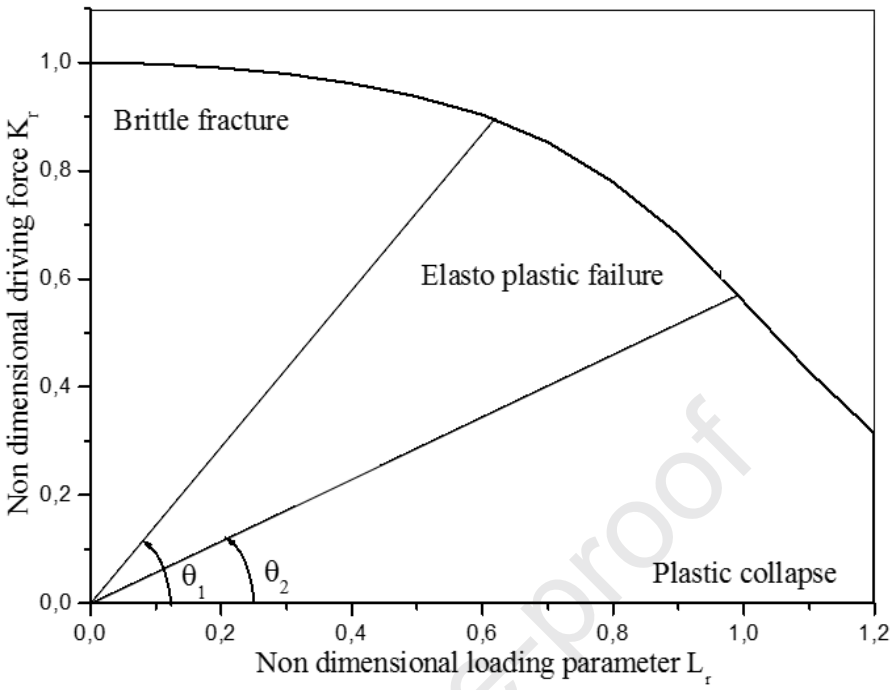

Fig. 7. The schematic view of the notch failure assessment diagram (NFAD) and three typical domains. Adapted and modified from [84].

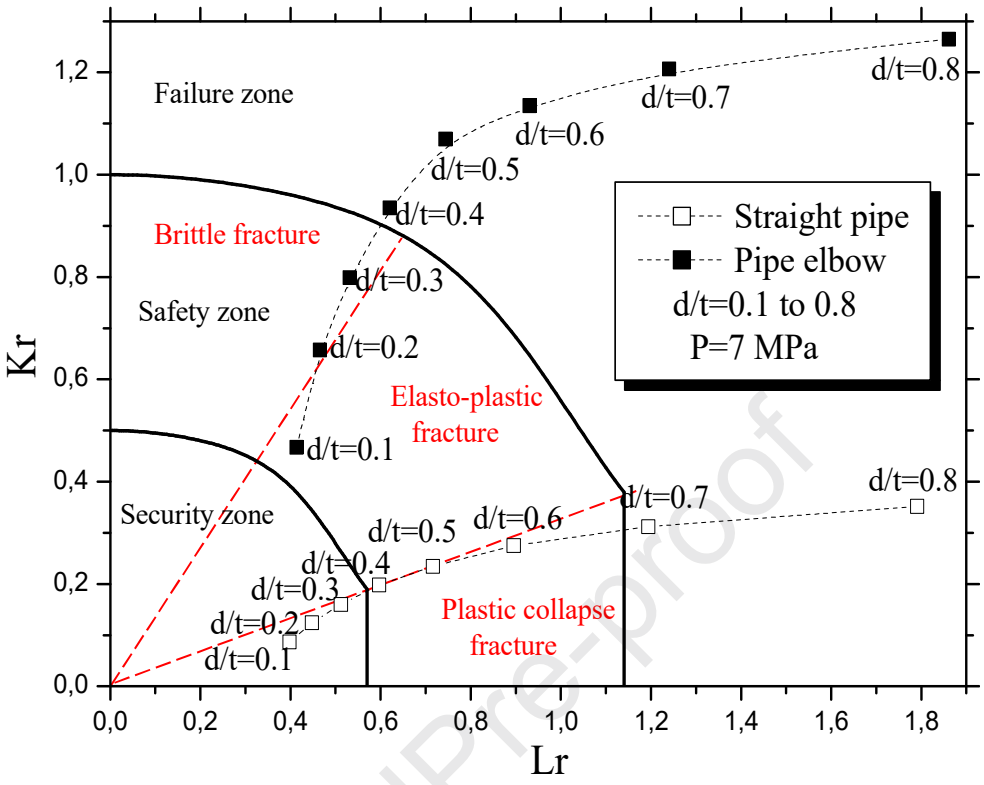

Fig. 8. Notch failure assessment diagram (NFAD) for the straight pipe and pipe elbow with different depth ratios (*d/t*= 0.1 - 0.8) of the rectangular parallelepiped-shaped corrosion defects with rounded corners at the intrados section.

Highlights

- Integrity of corroded pipe elbow was investigated based on the limit pressure.
- A parallelepiped rounded borders corrosion defect was created in the intrados section.
- The numerical finite element analyses (FEA) were done to modify the codes.
- Two models (modified B31G and DNV RP-F101) agrees well with FEA results.
- The notch failure assessment diagram (NFAD) confirms the pipe elbow criticality.

Declaration of interests

☒ The authors declare that they have no known competing financial interests or personal relationships that could have appeared to influence the work reported in this paper.

☐The authors declare the following financial interests/personal relationships which may be considered as potential competing interests: